2012 IEEE International Conference on Robotics and Automation
RiverCentre, Saint Paul, Minnesota, USA
May 14-18, 2012

Optimal Design of Nonlinear Profile of Gear Ratio using Non-circular Gear for Jumping Robot

Masafumi OKADA and Yushi TAKEDA

***Abstract*— In this paper, we develop a design method of nonlinear profile of gear ratio to utilize a DC servo motor effectively for a jumping robot. Because the larger ground force yields the higher kinetic energy of the robot body, the optimal gear ratio is obtained by the maximization of the ground force from statics point of view. Moreover, the varying gear ratio during the jump motion is obtained through a simulation which connects statics-based optimization and robot dynamics. A non-circular gear is synthesized which realizes the obtained optimal varying gear ratio. The effectiveness of the proposed method is evaluated by simulations.**

I. INTRODUCTION

For mechanical design of a robot system, a reduction gear is utilized generally to change the actuator property depending on the requirement of high torque output or high velocity realization. DC (Direct Current) motor is classified based on its power P[W] and the motor current and angular velocity have high correlation. The motor current yields output torque τ[Nm] and the relationship between τ and angular velocity ω[rad/sec] is represented by $\tau\omega = P$, which means that the motor torque τ will be small for the larger ω. By assuming the gear ratio as G, the output torque is multiplied by $1/G$ and the angular velocity is multiplied by G. So, an appropriate gear ratio has to be selected considering the robot tasks.

We consider a jumping robot. It requires (i) a high torque output to kick the ground in the beginning of the motion, on the other hand, (ii) high velocity realization in the end of the motion as shown in Fig.1. The lower gear ratio in (i) and the higher gear ration in (ii) are required. From these considerations, a varying gear ration will be necessary and appropriate nonlinear property of varying ration have to be optimally designed to jump higher with an effective use of a DC motor.

Many researches on jumping robots have been reported so far. Niiyama [1] realized a jump motion of a humanoid robot with musculoskeletal mechanism. Ishikawa [2] proposed a motion stabilization method of hopping robots based on hybrid-system control theory. Ugurlu [3] proposed a ZMP-based jumping controller design method. These are researches on control. Shimoda [4] and Sakaguchi [5] developed a jumping principal and mechanism using inertia force of a mass inside the body. Kovac [6], Curran [7] and Tsuda [8] proposed jumping mechanism using potential energy of a spring. These researches are on development of a mechanism and its control.

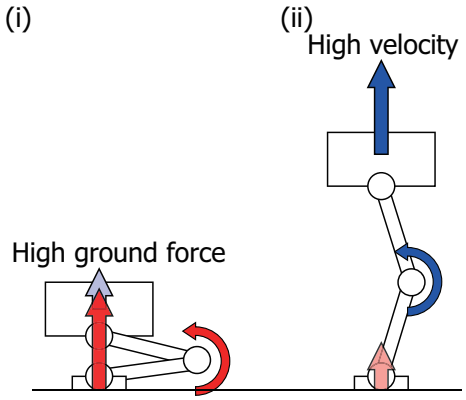

Fig. 1. Jumping robot property

It is true that the usage of a spring yields large height of jumping, however, it may consume large energy of actuator because not all the accumulated energy of the spring will be available. In this paper, aiming at an optimal use of an actuator efficiency, we design a nonlinear profile of the varying gear ratio for a jumping motion and synthesize a non-circular gear that realizes the designed gear ratio. The purposes of this paper are as follows;

1) Based on statics of the mechanism, an optimal gear ration that maximizes a ground force of a jumping robot is introduced.
2) To connect the statics-based optimal gear ratio to robot dynamics, a simulation-based design method of a varying gear ratio is proposed.
3) A non-circular gear that realizes the varying gear ratio is synthesized.
4) The effectiveness of the proposed design method is evaluated by simulations.

CVT (Continuously Variable Transmission) is used for a automobile transmission that realizes a varying gear ratio, however, it is for a multiple rotational actuator with high angular velocity. Hagiwara [9] and Takaki [10] proposed special mechanisms that realize load sensitive varying gear ratio. The proposed method in this paper focuses on a fixed but position depending gear ratio for a robot motion.

This research is supported by the "Research on Macro / Micro Modeling of Human Behavior in the Swarm and Its Control" under the Core Research for Evolutional Science and Technology (CREST) Program (Research area : Advanced Integrated Sensing Technologies), Japan Science and Technology Agency (JST).

M. Okada and Y. TAKEDA are with Dept. of Mechanical Sciences and Engineering, Tokyo TECH, 2-12-1 Ookayama Meguro-ku Tokyo, JAPAN okada@mep.titech.ac.jp, takeda.y.ac@m.titech.ac.jp

II. Optimization of gear ratio

In this section, the optimal value of the gear ratio is obtained based on statics. Consider a jumping robot as shown in Fig.2. This robot has one degree of freedom with one DC

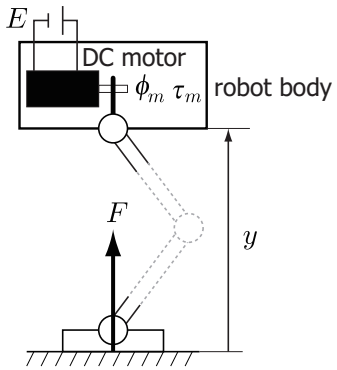

Fig. 2. Jumping robot

motor in the body, and the motor torque τ_m is transferred to the ground force F through a reduction gear and leg mechanism. The configuration of the leg mechanism is out of consideration in this section but its kinematics is assumed to be represented by;

$$y = f(\phi_m) \tag{1}$$

where ϕ_m and y represent the rotational angle of the motor and the body height respectively.

Because the kinetic momentum L of the robot body is calculated by

$$L = \int_0^{t_{off}} F dt \tag{2}$$

at the takeoff time t_{off}, the larger F maximizes the takeoff velocity of the body with the larger t_{off}. In the following, the gear ratio G (i.e. reduction ratio is G^{-1}) which maximizes the ground force F is obtained.

The power voltage is assumed to be E = constant. The motor current i satisfies the following equation from Kirchhoff's laws.

$$E = iR + L_m \frac{di}{dt} + K_a \dot{\phi}_m \tag{3}$$

where R represents a terminal resistance of the motor, L_m means a motor inductance, K_a means a torque constant (= back electromotive constant). By assuming L_m is negligible small, i is represented by;

$$i = \frac{1}{R}\left(E - K_a \dot{\phi}_m\right) \tag{4}$$

The output torque of the motor is obtained by;

$$\tau_m = K_a i = \frac{K_a}{R}\left(E - K_a \dot{\phi}_m\right) \tag{5}$$

On the other hand, kinematics of the mechanism represented in equation (1) yields

$$\dot{y} = \frac{\partial f}{\partial \phi_m}\dot{\phi}_m = J(\phi_m)\dot{\phi}_m \tag{6}$$

where J represents Jacobian matrix. Equation (6) shows the ratio of change between y and ϕ_m, which is represented by;

$$\frac{\dot{y}}{\dot{\phi}_m} = J(\phi_m) \tag{7}$$

which means that the gear ratio G from the rotational angle of motor ϕ_m to the body height y is represented by;

$$G = J(\phi_m) \tag{8}$$

Moreover the relationship between τ_m and F is represented by

$$F = J^{-1}\tau_m = G^{-1}\tau_m \tag{9}$$

from virtual work principle.

By substituting equations (5) and (6) into (9), the ground force is represented by

$$F = G^{-1}\frac{K_a}{R}\left(E - K_a G^{-1}\dot{y}\right) \tag{10}$$

Asumming $\dot{y} > 0$, equation (10) is a quadratic function of convex upward with respect to G^{-1}, and there exists an optimal G^{-1} that maximize F as;

$$G^{-1} = \frac{E}{2K_a\dot{y}} \tag{11}$$

In a jumping motion, $\dot{y} \geq 0$ is always satisfied without loss of generality. In this paper, the varing gear ratio is realized by a non-circular gear, which means G has to be a function of ϕ_m, however, equation (11) represents that the optimal G is a function of $\dot{y}$. Thus the relationship between ϕ_m and $\dot{y}$ has to be obtained as $\dot{y} = \dot{y}(\phi_m)$. In the next section, a simulation-based method to connect $\dot{y}$ and ϕ_m is proposed. Though the proposed simulation-based method connects statics (optimal gear ratio) and dynamics (rerationship between $\dot{y}$ and ϕ_m), it contains time integral of the dynamics of the specified mechanism with a specified initial value, which means the obtained varying gear ratio is optimal only for one mechanism and one initial value of the jumping motion.

III. Jumping robot and its dynamics

A. Robot mechanism

To obtain the solution of $\dot{y} = \dot{y}(\phi_m)$, a simulation-based method is utilized. In this section, one jumping robot is specified and its dynamical model is introduced. Consider a jumping robot mechanism as shown in Fig.3. The motor torque τ_m is transferred to the rotational torque τ_1 of the leg through three gears. The gear ratio of each gears are defined as G_1, G_2 and G_3 respectively. G_1 and G_3 are constant values. G_2 has varying property because Gear2 is a non-circular gear. G_2 is a design parameter. Gear1 amplifies the motor torque with a large value of reduction ratio G_1^{-1}. Gear3 is for adjustment of the rotation of Gear2 ($0 \sim 1.5\pi$ rad will be appropriate for the rotation of Gear2 through the motion).

Two links of the leg have same length 2ℓ and they moves with the constrain;

$$\theta_1 + \theta_2 = \pi \tag{12}$$

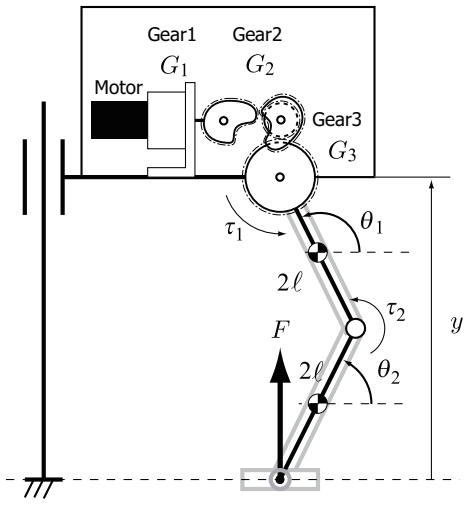

Fig. 3. Jumping robot model

where θ_1 and θ_2 are absolute rotational angles of each link. Fig.4 shows one example of the leg mechanism [11] that satisfies the constrain in equation (12). This mechanism

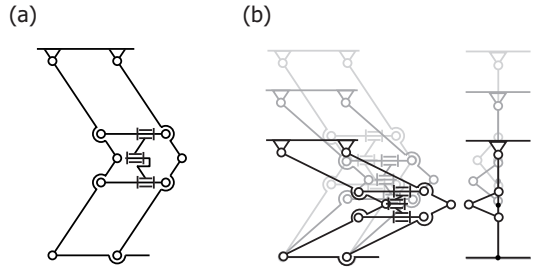

Fig. 4. Leg mechanism with closed kinematic chain

has two parallelograms, and 3D closed kinematic chain constrains the body motion vertically with one degree of freedom.

B. Robot dynamics and optimization of gear ratio

By considering joint force and torque, Euler's motion equation is obtained. Here we remark that;

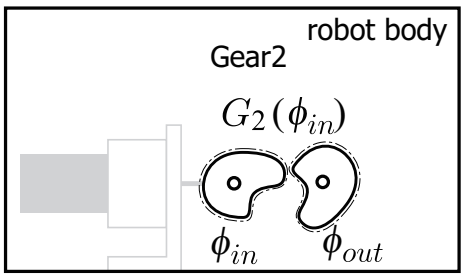

Fig. 5. Non-circular gear in Gear2

1) As shown in Fig.5, gear ratio G_2 is defined by the rotational angle of the input gear ϕ_{in} as;

$$G_2 = G_2(\phi_{in}) \tag{13}$$

The relationship between the angular acceleration of the rotations of the output gear ϕ_{out} and input gear ϕ_{in} are represented by

$$\ddot{\phi}_{out} = G_2\ddot{\phi}_{in} + \frac{dG_2}{d\phi_{in}}\dot{\phi}_{in}^2 \tag{14}$$

because ϕ_{out} is represented by

$$\phi_{out} = \int G_2(\phi_{in})\ d\phi_{in} \tag{15}$$

2) In this mechanism, equation (11) is changed as

$$\{J_\ell(\theta_1)G_3G_2G_1\}^{-1} = \frac{E}{2K_a\dot{y}} \tag{16}$$

$$J_\ell(\theta_1) = \frac{\partial y}{\partial \theta_1} = 4\ell\cos\theta_1 \tag{17}$$

and the optimal value of reduction ratio G_2^{-1} that maximizes the ground force F is obtained by;

$$G_2^{-1}(\phi_{in}) = \frac{EJ_\ell(\theta_1)G_1G_3}{2K_a\dot{y}} \tag{18}$$

where J_ℓ is Jacobian matrix of the leg mechanism represented by;

$$\dot{y} = J_\ell\dot{\theta}_1 \tag{19}$$

By executing a simulation with an initial value of θ_1, we obtain $\dot{y}[k]$ and $\theta_1[k]$ in each sampling step k and $G_2[k]$ is obtained from equation (18). The simulation also gives $\phi_{in}[k]$ and $\phi_{out}[k]$ from equation (15) and rotational ratio of $\phi_{in}[k]$ and $\phi_{out}[k]$ is obtained as shown in Fig.6, which gives the pitch curve of non-circular giear.

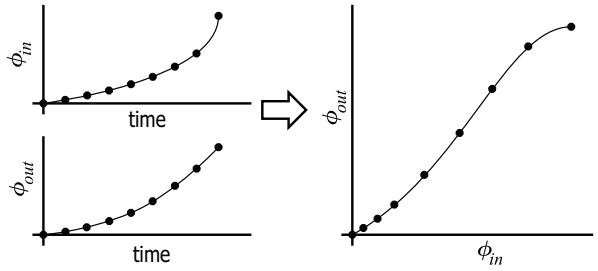

Fig. 6. Rotational ratio between ϕ_{in} and ϕ_{out} from simulation data

IV. Design of Gear Ratio with Jumping Simulation

A. Design of varying gear ratio and non-circular gear

The power voltage E is set as 24V and the initial value of θ_1 is set as $179°$ ($\theta_2 = 1°$). Supposing 60W DC servo motor (MAXON Corp.), $R = 1.53\Omega$, $K_a = 39.8 \times 10^{-3}$Nm/A are selected. $G_1 = 1/100$ (for example, HarmonicDrive gear will be utilized), $G_3 = 1/5$, $\ell = 0.2$m (leg length $= 0.4$m) and robot weight $M = 2.5$kg are set. Though the optimal reduction ratio G_2^{-1} was discussed in equation (18), the small value of $\dot{y}$ yields extremely large value of G_2^{-1}, which cannot be realized by a non-circular gear. Thus in this paper, G_2^{-1} is bounded by $G_2^{-1} \leq 3$. The viscous friction of Gear1 is considered and the upper limit of the motor current is set as $i \leq i_{max} = 10$A.

For the simulation, $dG_2/d\phi_{in}$ in equation (14) is necessary, but it is not obtained a prior because G_2 is obtained in each sampling step. By using the difference ΔG_2 and $\Delta\phi_{in}$ defined by;

$$\Delta G_2 = G_2[k] - G_2[k-1] \quad (20)$$

$$\Delta\phi_{in} = \phi_{in}[k] - \phi_{in}[k-1] \quad (21)$$

from the obtained G_2 and ϕ_{in} in each sampling step, $dG_2/d\phi_{in}$ is approximated by;

$$\frac{dG_2}{d\phi_{in}} = \frac{\Delta G_2}{\Delta\phi_{in}} \quad (22)$$

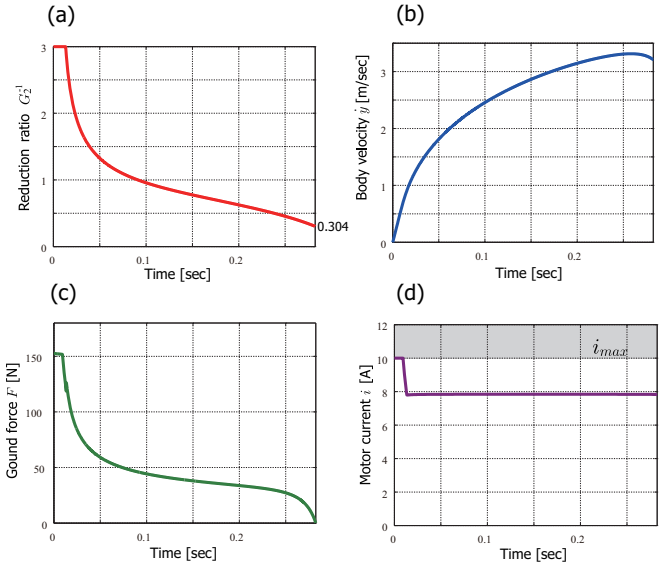

Fig. 7. Time variations of G_2^{-1}, $\dot{y}$, F and i in the jumping simulation

Under these conditions, the jumping simulation is executed. The takeoff time t_{off} is calculated by the condition of $F \leq 0$ and the body velocity $\dot{y}_{off}$ is obtained as;

$$\dot{y}_{off} = 3.21 \text{ m/sec} \quad (23)$$

Fig.7 shows the time variations of (a) reduction ratio G_2^{-1},

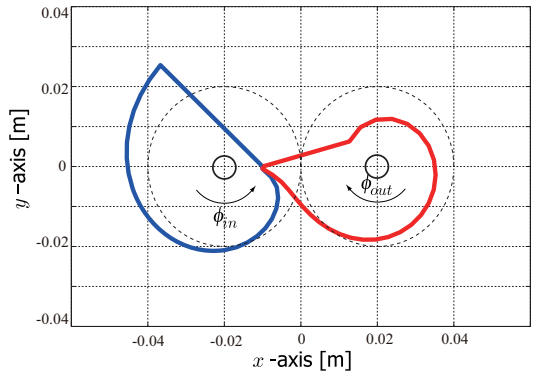

Fig. 8. Shape of the pitch curve of the non-circular gear

(b) body velocity $\dot{y}$, (c) ground force F and (d) motor current i in the simulation. In the beginning of the motion, G_2^{-1} is equal to 3 which is the upper limit of G_2^{-1} because of the small value of $\dot{y}$. After that, G_2^{-1} is optimized with increasing $\dot{y}$. The motor current is restricted by $i \leq i_{max}$ in the beginning of the motion. After G_2 is optimized, i converges a constant value ($\simeq$ 8A). The ground force takes a large value in the beginning of the motion, and gradually changes to small value until it reaches zero at $t = t_{off} = 0.283$ sec. The rotational angle of the leg $\theta_1 = 114°$ at $t = t_{off}$.

Based on the simulation result, a non-circular gear that realizes the optimal gear ratio is synthesized. By setting the distance between the input and output gear axes as r, the radius of the input gear r_{in} is calculated as;

$$r_{in}(\phi_{in}) = \frac{r}{1 + G_2^{-1}(\phi_{in})} \quad (24)$$

where ϕ_{in} is the rotational angle of the input gear. Fig.8 shows the shape of the pitch curve of the non-circular gear. r is set as $r = 0.04$m.

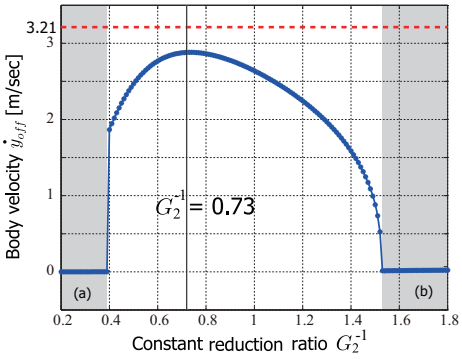

Fig. 9. The relationship between constant G_2^{-1} and $\dot{y}_{off}$

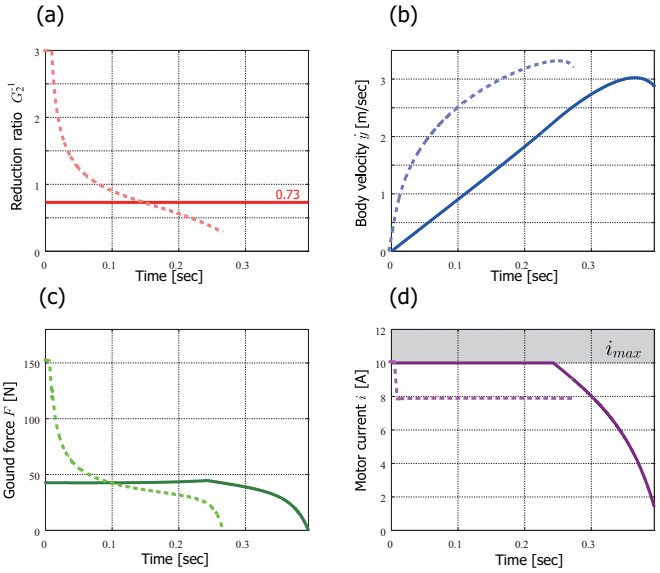

Fig. 10. Time variation of G_2^{-1}, $\dot{y}$, F and i with constant gear ratio $G_2^{-1} = 0.73$

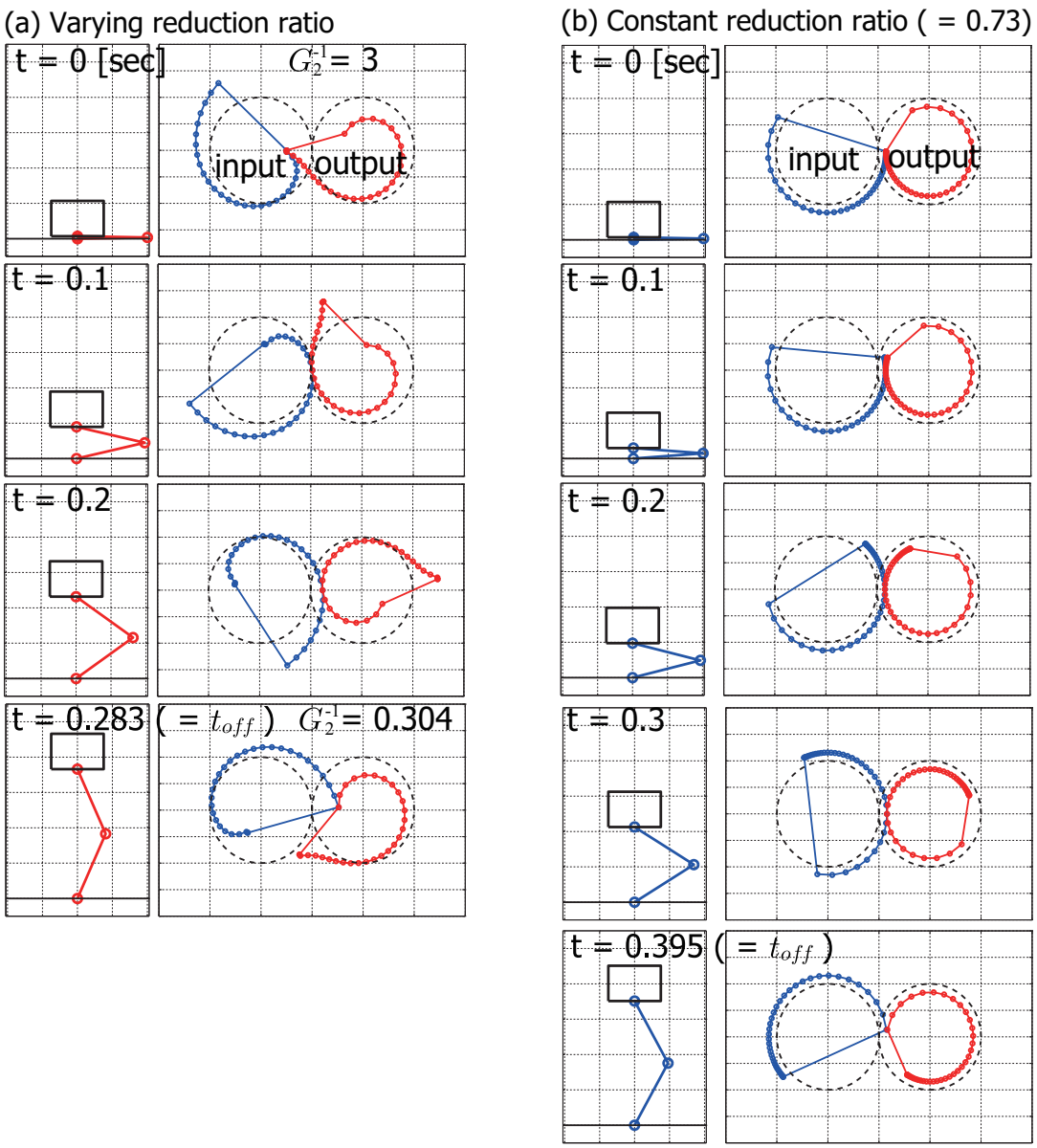

Fig. 11. Motion of the robot and gear

B. Comparison with constant gear ratio

To evaluate the effectiveness of the varying gear ratio, the maximum $\dot{y}_{off}$ is calculated by using a constant gear ratio using a circular gear. G_2^{-1} is set to a constant value and jumping simulation is executed. Fig.9 shows the relationship between G_2^{-1} and $\dot{y}_{off}$. G_2^{-1} is set from 0.2 to 1.8, and $\dot{y}_{off}$ is obtained for each G_2^{-1}. In area (a : $0.2 \leq G_2^{-1} \leq 0.39$), the robot cannot stand up from the initial value because of the low torque with the low reduction ratio. In area (b : $1.53 \leq G_2^{-1} \leq 1.8$), the robot cannot take off the ground because of the low velocity with the high reduction ratio. The red dashed line represents $\dot{y}_{off}$ with the optimal gear ratio in the previous section. $\dot{y}_{off}$ is maximized by $G_2^{-1} = 0.73$ and maximum value is $\dot{y}_{off} = 2.88$ m/sec. The rotation angle of the leg is $\theta_1 = 119°$ at $t_{off} = 0.395$sec. Same as Fig.7, the time variation of (a) G_2^{-1}, (b) $\dot{y}$, (c) F and (d) i using $G_2^{-1} = 0.73$ are shown in Fig.10. The dashed lines show the results in Fig.7 for comparison. Figure-(a) means that G_2^{-1} is constant ($= 0.73$). From figure-(b), we can see that the change of $\dot{y}$, i.e. the acceleration of the body is small by using a constant G_2^{-1} in the beginning of the motion, which means $G_2^{-1} = 0.73$ is too small for standing up motion. Figure-(d) shows the shortage of the motor current because i is almost bounded by i_{max} through the motion. Fig.11 shows the motion of the robot and rotation of the gear using varying gear ratio (figure-(a)) and constant reduction ratio $G_2^{-1} = 0.73$ (figure-(b)). In the beginning of the motion, the robot moves slowly in figure-(b) because of the low reduction ratio ($= 0.73$), on the other hand, the robot moves fast in figure-(a) with high reduction ratio ($= 3$).

However, the low reduction ratio is required in the end of the motion for high speed jump, which means $G_2^{-1} = 0.304$ (final value of varying G_2^{-1}) is appropriate in figure-(a) but $G_2^{-1} = 0.73$ is too large in figure-(b). This result shows the effectiveness of the varying gear ratio. The attached video shows the motion of the robot in Fig.11-(a) and (b). The upper movie shows the motion of the robot with the non-circular gear (Fig.11-(a)) and the lower movie shows that with the constant gear (Fig.11-(b)).

C. Discussions

From the simulation results, we can discuss as follows;

1) By using the optimized varying gear ratio, the robot obtains large takeoff body velocity which cannot be obtained by a constant gear ratio. The jumping height is calculated as 0.53m in regard to the maximum height 0.42m with a constant gear ratio, which is about 24% increase.
2) From equation (11),

$$G\dot{y} = \frac{E}{2K_a} (= \text{const.}) \tag{25}$$

is obtained. Moreover, by substituting equations (6) and (8) into equation (4), the motor current i is calculated as;

$$i = \frac{E}{2R} (= \text{const.}) \tag{26}$$

This value is smaller than i_{max} in this simulation (see Fig.7-(d)). However, by using a constant gear ratio, more motor current than i_{max} is required (see Fig.10-(d)). From these results, we can see that the optimized varying gear ratio realizes the effective use of motor performance.
3) Equation (25) causes $\dot{\phi}_m$ =constant which corresponds to $\dot{\phi}_{in}$ = constant. This result means that the motor and input gear rotate by constant angular velocity and the ground force is maximized by the change of G_2. From these considerations, we can see that the effectiveness of the actuator efficiency is caused by the mechanical design (design of the non-circular gear).
4) Fig.10-(d) shows that the constant gear ratio consumes more energy than the non-circular gear because the power voltage E is constant. It is because more energy is consumed not only for motor heating but also the motion energy of the rotation of the actuator (motor inertia). In section IV-B, we discussed that the constant $G_2^{-1} = 0.73$ is too small for the beginning of the motion, however, $G_2^{-1} = 0.73$ is too large in the end of the motion. From these considerations, we can conclude that the varying reduction ratio from high to low through the motion realizes the effective use of the motor performance.

V. Conclusions

In this paper, we focus on a jumping robot and the optimal design method of a nonlinear profile of varying gear ratio is proposed. Moreover the obtained gear ratio is realized by a non-circular gear. The results are as follows;

1) The varying gear ratio is optimized by maximizing the ground force. It is based on statics of the mechanism.
2) Through a simulation, the connecting method between statics-based optimization and the robot dynamics is proposed.
3) Based on the simulation results, the non-circular gear is synthesized.
4) The effectiveness of the proposed method is shown by the jumping simulations from the jumping height and motor current point of views.

References

[1] R. Niiyama and Y. Kuniyoshi : "Design of a Musculoskeletal Athlete Robot : A Biomechanical Approach", Proc. of 12th International Conference on Climbing and Walking Robots and the Support Technologies for Mobile Machines (CLAWAR 2009), pp.173–180, 2009.

[2] M. Ishikawa, A. Neki, J. Imura and S. Hara : "Energy preserving control of a hopping robot based on hybrid port-controlled Hamiltonian modeling", IEEE Conference on Control Applications (CCA2003), Paper No. CF-002507, 2003.

[3] B. Ugurlu, A. Kawamura : "Real-time Running and Jumping Pattern Generation for Bipedal Robots based on ZMP and Euler's Equations", Proc. of the IEEE/RSJ International Conference on Intelligent Robots and Systems, pp.1100–1105, 2009.

[4] S. Shimoda, T. Kubota and I. Nakatani : "New Mobility System Based on Elastic Energy under Microgravity", Proc. of the 2002 IEEE International Conference on Robotics and Automation, pp. 2296–2301, 2002.

[5] K. Sakaguchi, T. Sudo, N. Bushida, Y. Chiba, Y. Asai and K. Kikuchi : "Wheel-Based Stair-climbing Robot with Hopping Mechanism - Fast Stair-climbing and Soft-landing by Vibration of 2-DOF system -", JSME Journal of Robotics and Mechatronics, Vol.19, No.3, pp.258–263, 2007.

[6] M. Kovac, M. Fuchs, A. Guignard, J.C. Zufferey and D. Floreano : "A miniature 7g jumping robot", Proc. of the 2008 IEEE International Conference on Robotics and Automation, pp.373–378, 2008.

[7] S. Curran and D. E. Orin : "Evolution of a Jump in an Articulated Leg with Series-Elastic Actuation", Proc. of the 2008 IEEE International Conference on Robotics and Automation, pp.352–358, 2008.

[8] T. Tsuda, H. Mochiyama and H. Fujimoto : "A Compact Kick-and-Bounce Mobile Robot powered by Unidirectional Impulse Force Generators", Proc. of the 2009 IEEE/RSJ International Conference on Intelligent Robots and Systems, pp.3416–3421, 2009.

[9] T. Hagiwara and S. Hirose : "Development of Dual Mode X-Screw : A Novel Load-Sensitive Linear Actuator with a Wide Transmission Range", Proc. of the 1999 IEEE International Conference on Robotics and Automation, pp.537–542, 1999.

[10] T. Takaki, K. Sugiyama, T. Takayama and T. Omata : "Development of two DOF finger using load-sensitive continuously variable transmissions and ultrasonic motors", Advanced Robotics, Vol.20, No.8, pp. 897–911, 2006.

[11] M. Okada and K. Murakami: "Robot Communication Principal by Motion Synchronization using Orbit Attractor", Proc. of the IEEE International Conference on Robotics and Automation (ICRA'07), pp.2564–2569, 2007.